

Real-Time Tracking of Phytochrome's Orientational Changes During Pr Photoisomerization

Yang Yang,^{†,||} Martin Linke,[†] Theodore von Haimberger,[†] Janina Hahn,[‡] Ricardo Matute,^{§,⊥} Leticia González,[§] Peter Schmieder,[‡] and Karsten Heyne^{*,†,||}

[†]Department of Physics, Freie Universität Berlin, Arnimallee 14, 14195 Berlin, Germany

[‡]Leibniz-Institut für Molekulare Pharmakologie, Robert-Rössle Str. 10, 13125 Berlin, Germany

[§]Institut für Physikalische Chemie, Friedrich-Schiller Universität Jena, Helmholtzweg 4, 07743 Jena, Germany

^{||}Center for Supramolecular Interactions, Takustr. 3, 14195 Berlin, Germany

[⊥]Departamento de Química, Universidad de Chile, Facultad de Ciencias, Casilla 653, Santiago, Chile

Supporting Information

ABSTRACT: Photoisomerization of a protein bound chromophore is the basis of the light sensing and signaling responses of many photoreceptors. *Z*-to-*E* photoisomerization of the Pr Cph1Δ2 phytochrome has been investigated by polarization resolved femtosecond visible pump-infrared probe spectroscopy, which yields structural information on the Pr excited (Pr*), Pr ground, and lumi-R product states. By exhaustive search analysis, two photoreaction time constants of (4.7 ± 1.4) and (30 ± 5) ps were found. Ring D orientational change in the electronic excited state to the transition state (90° twist) has been followed in real-time. Rotation of ring D takes place in the electronically excited state with a time constant of 30 ± 5 ps. The photoisomerization is best explained by a single rotation around C₁₅=C₁₆ methine bridge in the Pr* state and a diffusive interaction with its protein surrounding.

Phytochromes¹ are a family of dimeric chromoproteins that absorb light by means of a bound bilin (or linear tetrapyrrole) chromophore and regulate numerous photoresponses in plants, bacteria, and fungi.^{1–4} They sense red and far-red light by means of two relatively stable conformers: a red light absorbing Pr form with ZZZssa (C₅-Z, C₁₀-Z, C₁₅-Z, C₅-syn, C₁₀-syn, C₁₅-anti, Figure 1, inset) chromophore geometry^{2,3,5–9} and a far-red light absorbing Pfr form with a ZZEssa chromophore conformation.³ By photoconversion between active and inactive forms, phytochromes act as light-regulated master switches for measuring the fluence, direction, and color of the ambient light. Light absorption by the stable Pr form triggers an ultrafast *Z*-to-*E* isomerization of the C₁₅=C₁₆ methine bridge between the C and D rings of the bilin chromophore accompanied by rotation of ring D (Figure 1, inset).^{10–12} The structural switch initially localized at the bilin chromophore is cascaded via intramolecular couplings to slower and widespread structural changes which finally lead to the Pfr form.^{10,13–15} Excitation of the Pfr form initiates the ultrafast *E*-to-*Z* isomerization of the bilin chromophore, which finally leads to the Pr form.^{16,17} Even though both photoreactions are backreactions of each other, Pr to Pfr and Pfr to Pr reactions

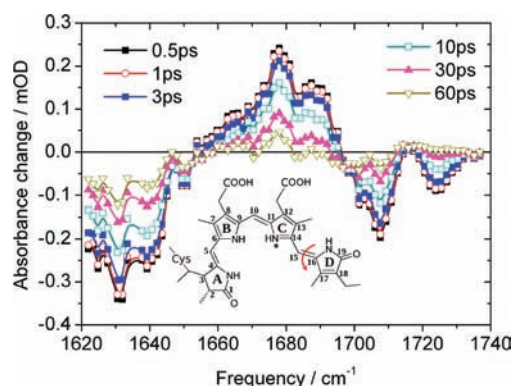


Figure 1. Isotropic absorbance difference of Pr phytochrome in the frequency range of $\nu(\text{C}=\text{O})$ stretching vibrations after excitation at 660 nm for different delay times. The spectral signal is calculated by $(A_{\parallel} + 2A_{\perp})/3$ from the two individual data points of the transient. Inset: PCB chromophore of Cph1Δ2 with ZZZssa geometry. The red arrow indicates our proposed counter-clockwise isomerization around C₁₅=C₁₆ double bond.

are completely different photoreactions, since they do not share intermediate states.

Unfortunately, only a few spectroscopic methods allow for the direct tracking of fast structural and orientational changes in proteins on a nanosecond time scale.¹⁸ From direct and indirect methods it is known that the chromophore in photoreceptors such as rhodopsin, bacteriorhodopsin, and photoactive yellow protein isomerizes around a C=C double bond on a time scale of 0.2–3 ps.^{19–21} Phytochrome Pfr photoreaction shows time constants in the range of 0.2–4 ps suggesting a similar reaction mechanism.^{12,22,23} Since both phytochrome Pfr and Pr photoreactions involve isomerization of the C₁₅=C₁₆ methine bridge and occur in the same protein environment one would expect similar reaction dynamics. In contrast, the primary photoisomerization of the Pr form of plant and bacterial phytochromes exhibits isomerization time constants in the range of 3–16 and 25–40 ps,^{6,14,22,24–28} followed by lumi-R photoproduct formation with quantum yields in the range of

Received: October 6, 2011

Published: January 9, 2012

7–16%.^{6,15,22,25–27} Despite the kinetic insight gained from these femtosecond time-resolved electronic and vibrational investigations, it was not possible to establish when the C₁₅=C₁₆ double bond isomerization and the ring D rotation occur, and what kind of structural changes the lumi-R photoproduct exhibits. This is due to the fact that traditional femtosecond time-resolved infrared and Raman spectroscopic methods provide important information on structural dynamics^{6,19,26} but are not able to track orientational changes of vibrational transition dipole moments (tdm) in real time.

In this study, we used polarization resolved femtosecond visible pump infrared probe (prfs VIS-IR) spectroscopy^{29,30} to determine the orientation of the $\nu(\text{C}_{19}=\text{O})$ vibrational modes on a femtosecond time scale in the Pr* and Pr state. Prfs VIS-IR spectroscopy provides direct transient information on the relative angle between the excited electronic transition dipole moment (tdm) and the probed vibrational tdm. The tdm's are fixed within the molecular scaffold of the chromophore, and their properties depend on the electronically excited state. To solely obtain signals from the chromophore's $\nu(\text{C}=\text{O})$ stretching vibrations, we used the phycocyanobilin (PCB) chromophore bound to ¹³C/¹⁵N-labeled Cph1Δ2 protein, where Cph1 is the cyanobacterial phytochrome from *Synechocystis* sp. PCC 6803 and Cph1Δ2 is the N-terminal 1–514 residue sensory module of Cph1, thus shifting all $\nu(\text{C}=\text{O})$, $\nu(\text{C}=\text{C})$, and $\nu(\text{C}=\text{N})$ stretching vibrations of the protein to lower frequencies and out of our spectral window of 1670–1745 cm⁻¹. All presented data were acquired under similar conditions. Excitation pulses were generated at 660 nm and attenuated to energies of 30 nJ to excite less than 3% of the Cph1Δ2 phytochrome sample.³¹ Simultaneously, two probe beams with parallel and perpendicular polarization with respect to the pump beam polarization were used to probe the transient changes in the sample with a time resolution better than 300 fs. The signals were recorded with a 2 × 32 element MCT array detector at a spectral resolution of 1.5 cm⁻¹. Thus, several measurements had to be performed to cover a spectral range from 1620–1740 cm⁻¹ as presented in Figure 1.

Structural changes initiated by the photoexcitation at 660 nm are reflected in changes in the chromophores' vibrational spectrum. Upon excitation, transient absorption signals were determined by the absorption signals with parallel A_{\parallel} and perpendicular A_{\perp} polarization, with respect to the pump pulse polarization. Isotropic signals were calculated according to $A_{\text{iso}} = (A_{\parallel} + 2A_{\perp})/3$. All transients were fitted best by a biexponential decay of (4.7 ± 1.4) and (30 ± 5) ps.^{6,12,15,22,26,27} The error margins represent 1 σ standard deviations as determined by exhaustive search analysis (ExSeAn).³²

In Figure 1 the negative ground-state recovery signal at 1631 cm⁻¹ represents signals of the PCB delocalized mode comprising the C₁₅=C₁₆ methine bridge and the C₁₇=C₁₈ double bond of the D ring,²⁶ with superimposed signals from ¹³C-labeled carbonyl modes of the protein. Frequencies above 1670 cm⁻¹ originate exclusively from chromophore $\nu(\text{C}=\text{O})$ stretching vibrations. Bleaching signals of the depleted ground state are negative, while excited state and product absorption show positive signals. Stimulated emission signals on vibrational transitions are negligible in this experimental setup. Signals and spectral shifts due to hot ground states or anharmonic couplings are not observed. The sharp dip at 1683 cm⁻¹ in Figure 1 is due to a nonlinear artifact attributed to interaction with water vapor. The decay of the $\nu(\text{C}_{19}=\text{O})^*$ stretching

vibration of ring D in the electronically excited state of Pr (Figure 1) has its maximum at 1680 cm⁻¹ and is red-shifted with respect to its ground-state absorption.^{24,33} The decay is governed by the 30 ps time constant (80%). The bleaching signals of the $\nu(\text{C}_{19}=\text{O})$ stretching vibration in the Pr ground state are located at 1708 cm⁻¹. At 1724 cm⁻¹, the ground-state recovery of the $\nu(\text{C}_1=\text{O})$ vibration of ring A is detected.^{10,34} The bleaching signal is superimposed with a lumi-R photoproduct absorption that arises after 40 ps.^{22,26}

Polarization resolved transients provide information on the angle between the S₀–S₁ electronic transition dipole moment vector (μ_{el}) and the probed vibrational transition dipole moment vectors (μ_{vib}) sketched in Figure 2.³⁵ From the

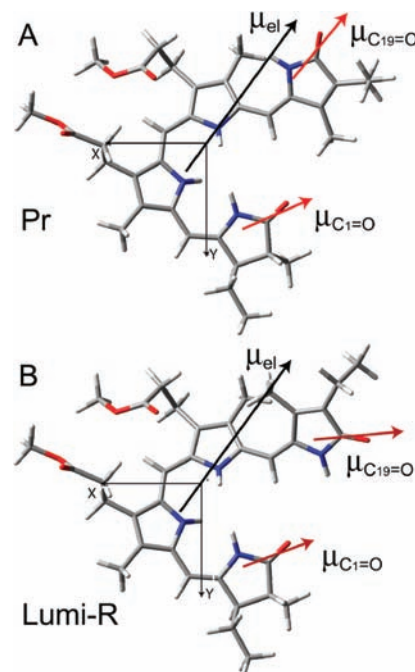


Figure 2. Calculated chromophore geometries for Pr ground state and lumi-R photoproduct and its electronic (black arrow) and vibrational (red arrows) tdm orientations.

dichroic ratio (DR), $\text{DR} = A_{\parallel}/A_{\perp}$, the angle ($\mu_{\text{el}}, \mu_{\text{vib}}$) between μ_{el} and μ_{vib} can be calculated as $(\mu_{\text{el}}, \mu_{\text{vib}}) = \arccos[(2 \text{DR} - 1)/(\text{DR} + 2)]^{1/2}$.

Evaluation of the first 6 ps of the polarization resolved transients at 1708, 1724, and 1680 cm⁻¹ in Figure 3 (see Supporting Information) reveals values for the angles of $(\mu_{\text{el}}^{\text{Pr}}, \mu_{\text{C}_{19}\text{O}}) = (17 \pm 7)^{\circ}$, $(\mu_{\text{el}}^{\text{Pr}}, \mu_{\text{C}_{10}}) = (47 \pm 4)^{\circ}$, and $(\mu_{\text{el}}^{\text{Pr}*}, \mu_{\text{C}_{19}\text{O}}) = (32 \pm 3)^{\circ}$, respectively. The angle for lumi-R at 1724 cm⁻¹ is calculated after 50 ps to be $(\mu_{\text{el}}^{\text{lumi-R}}, \mu_{\text{C}_{19}\text{O}}) = 62^{\circ}$ and an error range from 44° to 90°. The error range for this angle is bigger due to smaller signal strengths. By comparing measured relative angles for the Pr and lumi-R ground state with the calculated angles, we are able to verify structural models of the chromophore in the protein binding pocket. The calculated ZZZssa Pr geometry and the ZZEssa lumi-R geometry with its transition dipole moments are presented in Figure 2A,B. The calculated angles of the ZZZssa Pr geometry of $(\mu_{\text{el}}^{\text{Pr}}, \mu_{\text{C}_{19}\text{O}}) = 21^{\circ}$ and $(\mu_{\text{el}}^{\text{Pr}}, \mu_{\text{C}_{10}}) = 42^{\circ}$ and the ZZEssa lumi-R geometry of $(\mu_{\text{el}}^{\text{lumi-R}}, \mu_{\text{C}_{19}\text{O}}) = 61^{\circ}$ agree with the experimentally determined values.

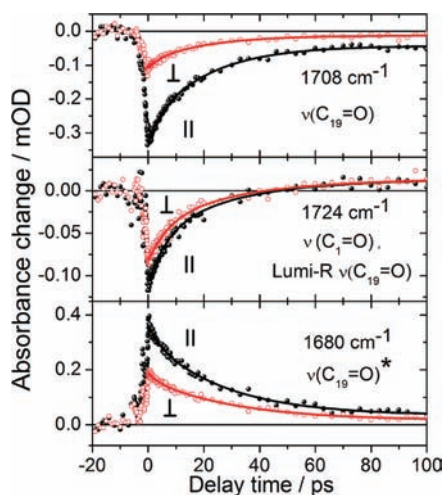


Figure 3. Polarization resolved transient absorptions of Cph1 Δ 2 phytochrome for parallel and perpendicular polarization at selected frequencies upon Pr photoexcitation. Errors are in the order of the point to point fluctuations.

The polarization resolved decay of the $\nu(\text{C}_{19}=\text{O})$ vibration in both its electronically excited states and its ground state are presented in Figure 4 on a logarithmic scale. Whereas the two

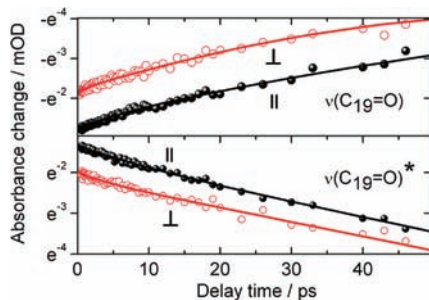


Figure 4. Polarization resolved transient signals and simulations on a logarithmic scale. Upper panel $\nu(\text{C}_{19}=\text{O})$ vibration and lower panel $\nu(\text{C}_{19}=\text{O})^*$ vibration. Upper panel: Identical slopes for parallel (||) and perpendicular (\perp) polarization indicate no change in dichroic behavior. Lower panel: Transient for parallel polarization (||) exhibits a steeper slope than that for perpendicular (\perp) polarization, demonstrating a change to greater angles. Point to point fluctuations indicate error margins.

decaying polarization resolved transients of the $\nu(\text{C}_{19}=\text{O})$ bleaching band in Figure 4 (upper panel) show a constant ratio, the ratio of the two polarization resolved transients in the electronically excited state changes over time. Therefore, the tdm of the $\nu(\text{C}_{19}=\text{O})^*$ vibration changes its average orientation in the electronically excited state from a dichroic ratio of $\text{DR}_0 = 1.94$ (31°) at time zero, to a $\text{DR}_{21} = 1.71$ (36°) at 21 ps, and finally to a $\text{DR}_{40} = 1.4$ (43°) at 40 ps (Figure 4 lower panel). This demonstrates that the Z-to-E photoisomerization of Pr phytochrome by rotation of ring D takes place in the electronically excited state on a time scale of tens of picoseconds, in contrast to earlier interpretations.²⁶ The average angle increases steadily up to 30 ps demonstrating ongoing isomerization dynamics in the electronically excited state on this time scale.

Assuming that all isomerizing chromophores reach a transition state in which ring D is twisted by 90° relative to

the plane of rings B and C and that all nonisomerizing chromophores maintain their planarity, the percentage of isomerizing chromophore molecules can be estimated by the decay of the DR. In the transition state, a twisted ring D has an angle between μ_{el} and $\nu(\text{C}_{19}=\text{O})^*$ vibrational tdm of about 90° and DR of 0.5, since μ_{el} lies in the average plane of rings B and C. Given the percentage of nonisomerizing chromophores x , dichroic ratio DR_0 and DR_{21} , the percentage of chromophores populating the transition state is about 16% at 21 ps delay time, when the amount of excited chromophores is halved, according to $x^*\text{DR}_0 + (1-x)^*0.5 = \text{DR}_{21}$. This result is in agreement with reported quantum yields of 7–16%.^{25,26}

Thus, our polarization resolved femtosecond vibrational data support an isomerization mechanism with a single isomerization around the $\text{C}_{15}=\text{C}_{16}$ double bond via a strongly twisted transition state.¹ An isomerization mechanism including an additional rotation around the $\text{C}_{14}-\text{C}_{15}$ single bond in the electronically excited state would result in negligible DR changes and is therefore less likely.^{13,15,36}

Real-time tracking of angular changes of the $\nu(\text{C}_{19}=\text{O})$ tdm provides direct information about the rotation of ring D but not on its direction of rotation. Nevertheless, additional information is available from the Pr crystal structure⁸ and the Pr and Pfr NMR structural data both in Cph1.⁹ In these structures ring D adopts α - and β -facial dispositions in Pr and Pfr forms, respectively. This agrees with CD experiments on the Pr and Pfr form of Cph1 in the longest wavelength absorption band.³⁷

If the $\text{C}_{19}=\text{O}$ group of ring D changed to the other side of the chromophore, it would have to pass significant energetic barriers due to steric interaction between the C_{13} methyl group of ring C and the N–H group of ring D in a first step and between the C_{13} methyl group of ring C and the C_{17} methyl group of ring D in the Pfr forming step. Therefore, it seems plausible that the $\text{C}_{19}=\text{O}$ group of ring D stays on the same side of the chromophore during counter-clockwise photoisomerization (as viewed from ring D side, Figure 1), forming lumi-R with a β -facial disposition.³⁷ During this process the $\text{C}_{19}=\text{O}$ group of ring D has to push His290 aside in a diffusive manner to reach the transition state. Consequently, the effective driving force for Pr photoisomerization is small, and the process thus slow.

We demonstrated real-time tracking of molecular orientational structural changes during the isomerization process in a photoreceptor. In the Pr form of Cph1 phytochrome ring D rotation around the $\text{C}_{15}=\text{C}_{16}$ double bond occurs in the electronically excited Pr* state with a time constant of 30 ps, much longer than the Pfr photoreaction. This demonstrates a distinct reaction mechanism for Pr photoisomerization, best explained by a diffusive mechanism. During rotation of ring D interaction with its protein surrounding makes isomerization strongly susceptible to structural changes in the electronic excited state.

The diffusive reaction mechanism on a time scale of tens of picoseconds allows tailoring of photoreaction quantum yield and reaction dynamics by modifying interaction partners of ring D in the protein binding pocket. These provide valuable insights for the field of photoreceptor engineering.

■ ASSOCIATED CONTENT

📄 Supporting Information

Materials and methods; experimental setup; calculations, and dichroic signals of transients. This material is available free of charge via the Internet at <http://pubs.acs.org>.

■ AUTHOR INFORMATION

Corresponding Author

karsten.heyne@fu-berlin.de

■ ACKNOWLEDGMENTS

We appreciate the support from the Deutsche Forschungsgemeinschaft (SFB 498 and GO 1059/2-1) and from the Center for Supramolecular Interactions, Free University Berlin. We thank M. P. Heyn and J. Hughes for valuable discussion on this work.

■ REFERENCES

- (1) Rockwell, N. C.; Su, Y. S.; Lagarias, J. C. *Annu. Rev. Plant Biol.* **2006**, *57*, 837.
- (2) Wagner, J. R.; Brunzelle, J. S.; Forest, K. T.; Vierstra, R. D. *Nature* **2005**, *438*, 325.
- (3) Hughes, J. *Biochem. Soc. Trans.* **2010**, *38*, 710.
- (4) Rockwell, N. C.; Lagarias, J. C. *Plant Cell* **2006**, *18*, 4.
- (5) Matute, R. A.; Contreras, R.; Pérez-Hernández, G.; González, L. J. *Phys. Chem. B* **2008**, *112*, 16253.
- (6) van Thor, J. J.; Ronayne, K. L.; Towrie, M. J. *Am. Chem. Soc.* **2007**, *129*, 126.
- (7) Hahn, J.; Strauss, H. M.; Schmieder, P. J. *Am. Chem. Soc.* **2008**, *130*, 11170.
- (8) Essen, L. O.; Mailliet, J.; Hughes, J. *Proc. Natl. Acad. Sci. U.S.A.* **2008**, *105*, 14709.
- (9) Song, C.; Psakis, G.; Langlois, K.; Mailliet, J.; Gärtner, W.; Hughes, J.; Matysik, J. *Proc. Natl. Acad. Sci. U.S.A.* **2011**, *108*, 3842.
- (10) Foerstendorf, H.; Benda, C.; Gärtner, W.; Storf, M.; Scheer, H.; Siebert, F. *Biochemistry* **2001**, *40*, 14952.
- (11) Siebert, F.; Grimm, R.; Rudiger, W.; Schmidt, G.; Scheer, H. *Eur. J. Biochem.* **1990**, *194*, 921.
- (12) Heyne, K.; Herbst, J.; Stehlik, D.; Esteban, B.; Lamparter, T.; Hughes, J.; Diller, R. *Biophys. J.* **2002**, *82*, 1004.
- (13) Matysik, J.; Hildebrandt, P.; Schlamann, W.; Braslavsky, S. E.; Schaffner, K. *Biochemistry* **1995**, *34*, 10497.
- (14) Sineshchekov, V. A. *Biochim. Biophys. Acta, Bioenerg.* **1995**, *1228*, 125.
- (15) Andel, F.; Hasson, K. C.; Gai, F.; Anfinrud, P. A.; Mathies, R. A. *Biospectroscopy* **1997**, *3*, 421.
- (16) Mroginiski, M. A.; Murgida, D. H.; von Stetten, D.; Kneip, C.; Mark, F.; Hildebrandt, P. J. *Am. Chem. Soc.* **2004**, *126*, 16734.
- (17) Rudiger, W.; Thummler, F.; Cmiel, E.; Schneider, S. *Proc. Natl. Acad. Sci. U.S.A.* **1983**, *80*, 6244.
- (18) Ihee, H.; Rajagopal, S.; Srajer, V.; Pahl, R.; Anderson, S.; Schmidt, M.; Schotte, F.; Anfinrud, P. A.; Wulff, M.; Moffat, K. *Proc. Natl. Acad. Sci. U.S.A.* **2005**, *102*, 7145.
- (19) Herbst, J.; Heyne, K.; Diller, R. *Science* **2002**, *297*, 822.
- (20) Schenkl, S.; van Mourik, F.; van der Zwan, G.; Haacke, S.; Chergui, M. *Science* **2005**, *309*, 917.
- (21) Wang, Q.; Schoenlein, R. W.; Peteanu, L. A.; Mathies, R. A.; Shank, C. V. *Science* **1994**, *266*, 422.
- (22) Muller, M. G.; Lindner, I.; Martin, I.; Gärtner, W.; Holzwarth, A. R. *Biophys. J.* **2008**, *94*, 4370.
- (23) Schumann, C.; Gross, R.; Wolf, M. M. N.; Diller, R.; Michael, N.; Lamparter, T. *Biophys. J.* **2008**, *94*, 3189.
- (24) Toh, K. C.; Stojkovic, E. A.; Rupenyana, A. B.; van Stokkum, I. H. M.; Salumbides, M.; Groot, M.-L.; Moffat, K.; Kennis, J. T. M. *J. Phys. Chem. A* **2011**, *115*, 11985.
- (25) Toh, K. C.; Stojkovic, E. A.; van Stokkum, I. H. M.; Moffat, K.; Kennis, J. T. M. *Proc. Natl. Acad. Sci. U.S.A.* **2010**, *107*, 9170.
- (26) Dasgupta, J.; Frontiera, R. R.; Taylor, K. C.; Lagarias, J. C.; Mathies, R. A. *Proc. Natl. Acad. Sci. U.S.A.* **2009**, *106*, 1784.
- (27) Schumann, C.; Gross, R.; Michael, N.; Lamparter, T.; Diller, R. *ChemPhysChem* **2007**, *8*, 1657.
- (28) Holzwarth, A. R.; Venuti, E.; Braslavsky, S. E.; Schaffner, K. *Biochim. Biophys. Acta* **1992**, *1140*, 59.
- (29) Heyne, K.; Mohammed, O. F.; Usman, A.; Dreyer, J.; Nibbering, E. T. J.; Cusanovich, M. A. *J. Am. Chem. Soc.* **2005**, *127*, 18100.
- (30) Lim, M.; Jackson, T. A.; Anfinrud, P. A. *Science* **1995**, *269*, 962.
- (31) Supporting Information.
- (32) Roelofs, T. A.; Lee, C. H.; Holzwarth, A. R. *Biophys. J.* **1992**, *61*, 1147.
- (33) Theisen, M.; Linke, M.; Kerbs, M.; Fidder, H.; Madjet, M. E. A.; Zacarias, A.; Heyne, K. *J. Chem. Phys.* **2009**, *131*, 124511.
- (34) van Thor, J. J.; Fisher, N.; Rich, P. R. *J. Phys. Chem. B* **2005**, *109*, 20597.
- (35) Linke, M.; Lauer, A.; von Haimberger, T.; Zacarias, A.; Heyne, K. *J. Am. Chem. Soc.* **2008**, *130*, 14904.
- (36) Fischer, A. J.; Lagarias, J. C. *Proc. Natl. Acad. Sci. U.S.A.* **2004**, *101*, 17334.
- (37) Rockwell, N. C.; Shang, L.; Martin, S. S.; Lagarias, J. C. *Proc. Natl. Acad. Sci. U.S.A.* **2009**, *106*, 6123.